

# Automated Construction of Variable Density Navigable Networks in a 3D Indoor Environment for Emergency Response

Submitted: 15<sup>th</sup> July 2015

Revised: 1<sup>st</sup> December 2015, 20<sup>th</sup> April 2016 and 10<sup>th</sup> August 2016

Pawel Boguslawski<sup>1,\*</sup>, Lamine Mahdjoubi<sup>1</sup>, Vadim Zverovich<sup>1</sup>, Fodil Fadli<sup>2</sup>

<sup>1</sup> Faculty of Environment and Technology, University of the West of England, Bristol, United Kingdom

<sup>2</sup> Department of Architecture and Urban Planning, College of Engineering, Qatar University, Doha, Qatar

\* Corresponding author, e-mail: [pawel.boguslawski@uwe.ac.uk](mailto:pawel.boguslawski@uwe.ac.uk)

Contact details:

Pawel Boguslawski

Department of Architecture and the Built Environment

Faculty of Environment and Technology

University of the West of England

Frenchay Campus, Coldharbour Lane

Bristol, BS16 1QY, United Kingdom

e-mail: [Pawel.Boguslawski@uwe.ac.uk](mailto:Pawel.Boguslawski@uwe.ac.uk)

e-mail: [pboguslawski@gmail.com](mailto:pboguslawski@gmail.com)

tel.: +44 1173287019

mobile: +44 7956044921

# 1 Automated Construction of Variable Density Navigable Networks in a 3D 2 Indoor Environment for Emergency Response

3 Pawel Boguslawski<sup>1,\*</sup>, Lamine Mahdjoubi<sup>1</sup>, Vadim Zverovich<sup>1</sup>, Fodil Fadli<sup>2</sup>

4 <sup>1</sup> Faculty of Environment and Technology, University of the West of England, Bristol, United Kingdom

5 <sup>2</sup> Department of Architecture and Urban Planning, College of Engineering, Qatar University, Doha,  
6 Qatar

7 \* Corresponding author, e-mail: pawel.boguslawski@uwe.ac.uk

## 8 Abstract

9 Widespread human-induced or natural threats on buildings and their users have made  
10 preparedness and rapid response crucial issues for saving human lives. The ability to identify the  
11 paths of egress during an emergency is critical for rescue and emergency services. Quality models  
12 supporting real, or near-real, time decision making and allowing the implementation of automated  
13 methods are very important. In this paper, we propose a novel automated construction of the  
14 Variable Density Network (VDN) for determining egress paths in ~~an emergency~~dangerous  
15 environments. VND is used for deriving a navigable network in an indoor building environment,  
16 including a full 3D topological model. The accuracy of the proposed paths prediction tool was  
17 compared with key methods for navigable network generation, using the actual floor plan of Doha  
18 World Trade Centre. Findings revealed that in comparison to prevailing approaches, a key benefit  
19 from this approach is an increased prediction accuracy of egress route planning.

20 **Keywords:** navigable networks, indoor navigation, emergency response, 3D modelling, topological  
21 models

## 22 1. Introduction

23 Destructive disasters caused by events such as fire, storm, or explosion result in damages and  
24 structural instability of buildings. Such disasters are rare but inevitable, and in the urban  
25 environment with high-rise and big public buildings they lead to casualties and occupants trapped  
26 inside. In this type of crisis, the challenge is to assist the search and rescue personnel in quickly  
27 preparing a plan to locate and rescue the surviving victims. Disasters such as the fire at Villagio  
28 shopping mall in Doha in May 2012, resulted in 19 people killed including 13 children, are reminders  
29 that effective preparedness and response might eliminate or reduce human errors and panic leading  
30 into the loss of lives (Scharfenort, 2012).

31 Tashakkori et al. (2015) emphasized the importance of situation awareness available for first  
32 responders in emergency response systems. The knowledge about indoor structure, occupancy or  
33 localization of fire utilities is minimal prior their arrival to the emergency scene. Thus, assessment of  
34 the scene and wrong decisions increase the response time. Therefore, actual and constantly updated  
35 information about the indoor situation, close outdoor area and optimal routes to selected points  
36 inside a building is crucial. This information includes, to name a few: floor plans, material types,  
37 location of hazardous materials, occupancy information, space ownership, location of water  
38 resources, fire and emergency utilities, etc.

39 In an emergency, up-to-date information is needed for coordination, communication and efficient  
40 decision making (DeCapua and Bhaduri, 2007). Availability of information about the indoor structure  
41 is critical for simulation of **emergency** movement of people and egress way finding for individual  
42 pedestrians and groups of people (Nelson and MacLennan, 1995; Pauls, 1995). Usually the focus is  
43 put on evacuation paths, flow of people and time necessary to leave a building (Kuligowski, 2004).  
44 However, the opposite paths, from outdoor to trapped people at certain locations in a building are  
45 taken by search and rescue teams. In such a scenario, a quick location of first responders and  
46 occupants is of great importance in search and rescue operations (Li et al., 2014). In the case of  
47 emergency, standard path finding using normal navigation routes may not be sufficient, as they may  
48 be too risky or not available due to damage (Liu and Zlatanova, 2012). In these circumstances, the  
49 ability for emergency and rescue personnel to identify alternative and optimal paths becomes  
50 critical.

51 Zverovich et al. (2016) proposed a new method for calculating safe paths taking hazard proximity  
52 into consideration. Standard navigable networks are not sufficient to perform hazard analysis. They  
53 include only connections available for pedestrians, whereas topological relations between adjacent  
54 rooms without doors in-between are not reflected. This applies not only for adjacency in horizontal  
55 direction but also vertical, through slabs. However, these connections are important in simulation of  
56 several hazard types, such as fire spread or explosion impact. Thus, 3D properties included in a  
57 model, e.g. spatial relationship in all directions, are essential for emergency response applications  
58 which go beyond evacuation path-finding.

59 This paper reports on the development of a new automated method for deriving a navigable  
60 network in a 3D environment, including full 3D topological model, which may be used for finding  
61 alternative egress routes and simulating phenomena associated with emergency **responsesituation**.  
62 The motivation of this research is to provide better situation awareness to the first responders prior  
63 to their arrival to the **emergency** scene.

### 64 **1.1. Navigable models**

65 Available navigable models in emergency response research focus on standard path finding using  
66 doors and corridors (Goetz and Zipf, 2011; Kwan and Lee, 2005; Liu and Zlatanova, 2012; Vanclooster  
67 et al., 2014; Yang and Worboys, 2015). Most of these approaches retrieve a navigable model from  
68 2D floor plans, while the 3D properties of the original environment are not always reflected in the  
69 model; even when the original 3D model is available. Very often, adjacent floors are connected only  
70 by vertical connections representing staircases, and spatial relationships between adjacent rooms  
71 sharing a ceiling/floor or a wall without a door are not reflected in these models. The resulting  
72 networks are often simplified in order to reduce the storage cost and improve path-finding  
73 computation time, which makes them unsuitable for alternative path finding or simulation of  
74 phenomena related to the emergency.

75 Various researchers propose more sophisticated models (Lamarche and Donikian, 2004; Lee, 2004;  
76 Liu and Zlatanova, 2012; Stoffel et al., 2007; Wenjie and Schneider, 2010), where a complex network  
77 is generated for special spaces intensively used for pedestrian navigation such as corridors or  
78 complex open spaces. This improves the navigable network within a building, because the original  
79 logical network, which reflects connections among adjacent rooms, is not an appropriate  
80 representation of navigation routes. The proposed automated methods are based on door and

81 concave corner locations and visibility (Liu and Zlatanova, 2012), Straight Medial Axis Transformation  
82 (Lee, 2004), Delaunay Triangulation spatial subdivision (Krūminaitė and Zlatanova, 2014; Lamarche  
83 and Donikian, 2004), and convex sub-regions partitioning (Stoffel et al., 2007). These methods often  
84 require input models with preserved consistency between the geometry and topology. In the case of  
85 incomplete or inaccurate floor plans, a network model may be interactively generated (Luo et al.,  
86 2014), but this may not be efficient in the case of emergency situations, when models for decision  
87 support should be available in a real or near-real time.

88 Indoor navigation including emergency navigation models have to meet several requirements  
89 (Brown et al., 2013; Wang and Zlatanova, 2013). Indoor spaces and their geometry included in an  
90 original building model should be classified based on predefined types and represented in the  
91 navigable model. Sub-division of spaces is one of the required functionalities, which makes the  
92 model suitable for accurate routing computation. Semantic information defining function, use or  
93 occupancy should be also reflected and attached to the relevant spaces. Static and moving objects  
94 that are obstacles for navigation are another elements, which should be incorporated in the model.  
95 Finally, connectivity among spaces based on their type has to be derived. These requirements are  
96 the most fundamental and are usually supplemented by other, more specific rules.

97

98 A slightly different approach to navigable network generation is utilized in robotic motion planning  
99 (Wallgrün, 2005). It is based on the Voronoi Diagram (VD) (Aurenhammer, 1991), where vertices and  
100 edges of the VD are used respectively to represent nodes and links in the network. This method may  
101 be used in an unknown environment, where the network is dynamically and automatically updated  
102 while the indoor scene is explored. Hierarchical structures are used to store networks in different  
103 granularity: from the coarsest to more detailed networks reflecting geometric details of the indoor  
104 environment. Different scales are used depending on required precision of path-planning.

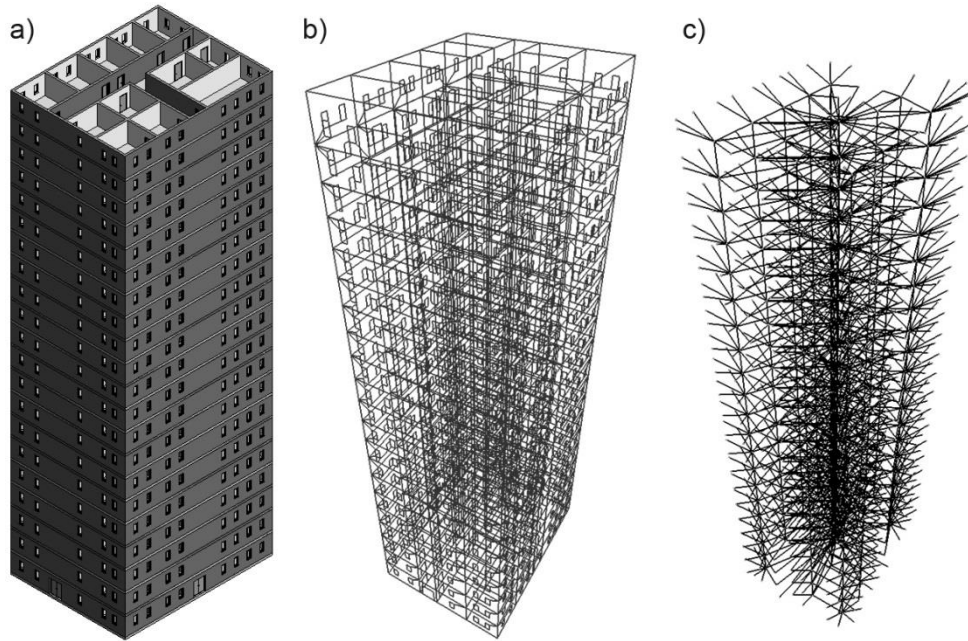
105 Higher level of granularity may be achieved through a network densification similar to mesh  
106 densification utilized in the finite element mesh generation and refinement (Du and Gunzburger,  
107 2002; Ho-Le, 1988; Petersen and Martins, 1997). Usually, mesh elements, e.g. triangles, are divided  
108 into smaller elements based on their centroids and original edges until the required level of  
109 granularity is achieved. Different criteria may be considered: the area of a mesh element or edge  
110 length. The size of the element is determined in a process (often iterative) minimizing an error  
111 between the exact solution and its finite element approximation (Du and Gunzburger, 2002; Dyck et  
112 al., 1992). A denser mesh may be generated locally in the vicinity of selected points (Chedid and  
113 Najjar, 1996).

114 Another field where densification of mesh is applied is geo-information: Triangulated Irregular  
115 Network (TIN), which is used to represent a digital model of terrain generated from point clouds and  
116 obtained from laser scanning. TIN is often densified using the Progressive TIN Densification (PTD)  
117 method (Axelsson, 2000; Zhang and Lin, 2013). New points are interpolated into a mesh  
118 representing the terrain which triggers division of a selected mesh triangle into smaller parts. The  
119 selection of a new point and the right triangle is based on specialized filters. Point candidates that do  
120 not belong to the terrain (e.g. buildings, trees, etc.) are calculated from their distance to TIN, and an  
121 angle between a mesh facet and a line connecting the point with the closest vertex of the facet.

122 Other models for indoor navigation systems are presented by Afyouni et al. (2012). The biggest  
123 drawback of these methods, in the context of applications other than standard indoor navigation, is  
124 that not all spatial relations among adjacent rooms are available in the model. Usually, 2D plans are  
125 used to reconstruct a navigable network within an individual building level. A link between two  
126 rooms is created only if they share a door. Otherwise, where adjacent rooms share a slab or wall  
127 without doors, adjacency relationship is not reflected in a model. Navigable networks for  
128 consecutive floors are connected at certain points by additional links representing staircases (Lee  
129 and Kwan, 2005).

130 However, some studies sought to fully utilise the 3D properties available from model reconstruction  
131 (Becker et al., 2009; Boguslawski et al., 2011). Their methods are based on the Poincaré duality: in  
132 practice the geometry of a volume is represented in the primal space using the boundary  
133 representation (B-Rep) (Stroud, 2006), while a volume object (e.g. a room) is represented as a dual  
134 node. A dual representation of a facet (e.g. a wall) is a dual edge bounded by dual nodes  
135 representing adjacent rooms – a link. Therefore, the dual structure is a graph of connections among  
136 3D objects. Attributes assigned to links may determine the navigability of the connections. These  
137 links with attributes form a sub-graph of the initial graph of connections and may be called a  
138 network.

139 The dual half-edge (DHE) proposed by Boguslawski (2011) is one of few data structures, which are  
140 able to simultaneously store both the primal and the dual graphs. The construction of a model is  
141 realized using CAD-like operators – Euler operators – where only the primal structure is explicitly  
142 constructed while the dual is automatically updated (Boguslawski and Gold, 2010). Figure 1 provides  
143 an example of a building represented with the DHE. In the model, doors and windows are  
144 represented as zero-volume objects with associated dual nodes, which are part of the graph;  
145 windows, which are embedded in a wall, are connected to the wall boundary using ‘bridge’ edges in  
146 order to fulfil B-Rep requirements and avoid disconnections in the graph. A characteristic property of  
147 the DHE model is the external volume enclosing the indoor model, which represents outside space.  
148 The indoor model can be combined with the terrain model or transportation network by the  
149 external cell (Boguslawski and Gold, 2015). The external volume is also considered in automatic exit  
150 detection: a door adjacent to internal and external volumes is marked as an exit.



151

152 Figure 1. A 3D model of a building represented with the DHE data structure: a) an original BIM  
 153 model; b) the DHE primal structure; c) the DHE dual graph of connections.

154 The dual graph, which reflects the adjacency relation between rooms, may be used to determine all  
 155 the neighbours of a certain room. This graph is a network: rooms are represented by dual nodes;  
 156 adjacent rooms are connected by a link; links can have different weights (i.e. attributes) associated  
 157 with each direction. The network may be used for indoor navigation: paths between two locations  
 158 can be calculated using graph algorithms (Boguslawski, 2011). A significant limitation of this  
 159 representation is its applicability only to simple models with ‘cubical’ rooms. Complex rooms need to  
 160 be manually partitioned into smaller sub-spaces with a specific configuration of doors in order to  
 161 produce a network suitable for accurate indoor navigation. This issue will be addressed in the  
 162 following section.

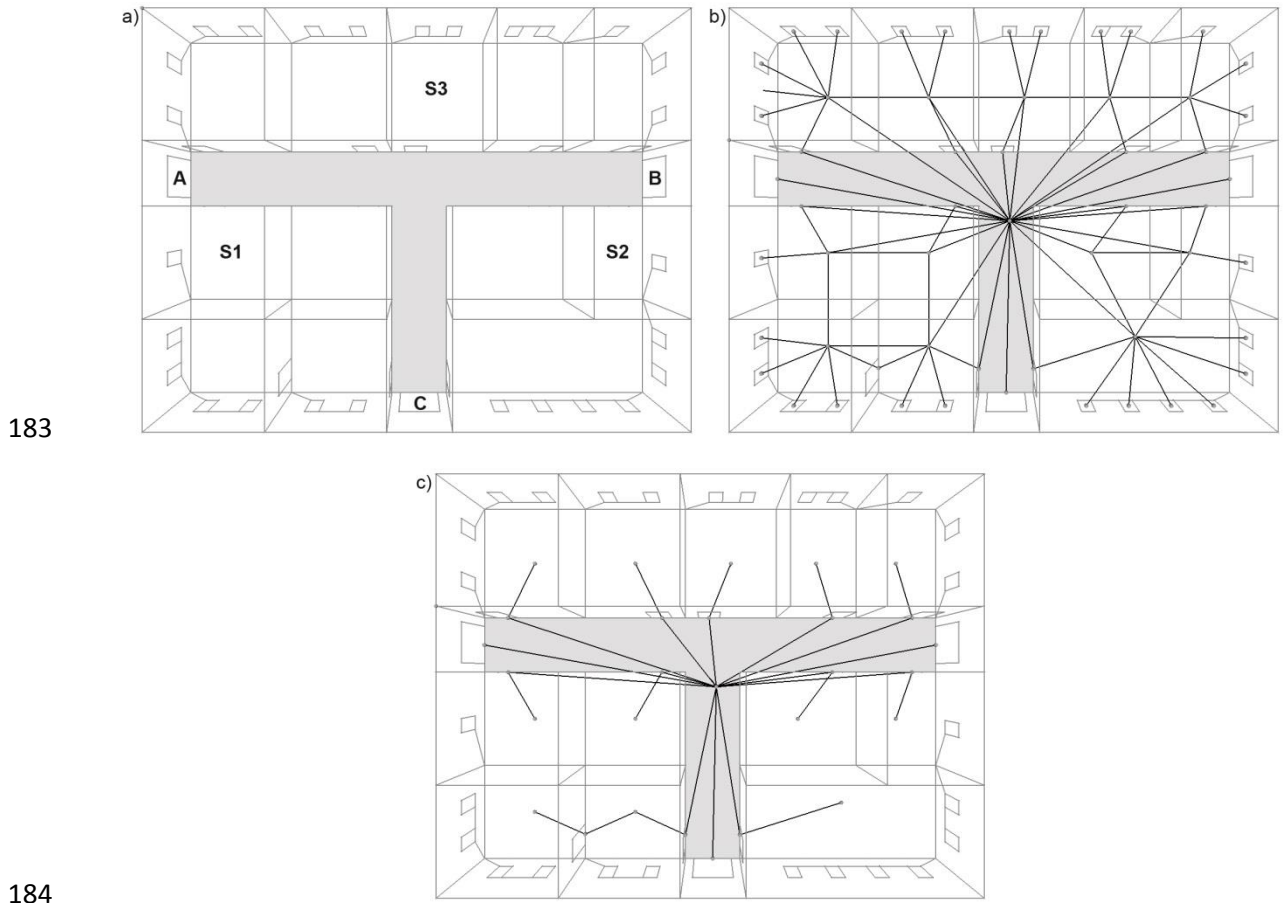
163 One of the advantages of the DHE representation is that not only links between adjacent rooms in  
 164 the horizontal direction are present in the model, but all possible adjacency relations are reflected  
 165 including those in the vertical direction. This is an important property, which is primarily used in  
 166 hazard propagation simulation. The possibility of vertical navigation through staircases is  
 167 automatically included in the model. Additionally, different weights for path-finding algorithms may  
 168 be attached to links going upstairs and downstairs.

169 Regardless of a method used for navigable network generation, in order to share the resulting  
 170 network and exchange between different applications, it should be represented in a common  
 171 schema. The IndoorGML (OGC, 2014) is a new standard designed for indoor navigation applications,  
 172 which complements other standards such as CityGML, KML and IFC. It consists of two main data  
 173 models: topology of indoor environment and indoor navigation, which describe a network topology  
 174 in built environment.

## 175 1.2. Problem statement

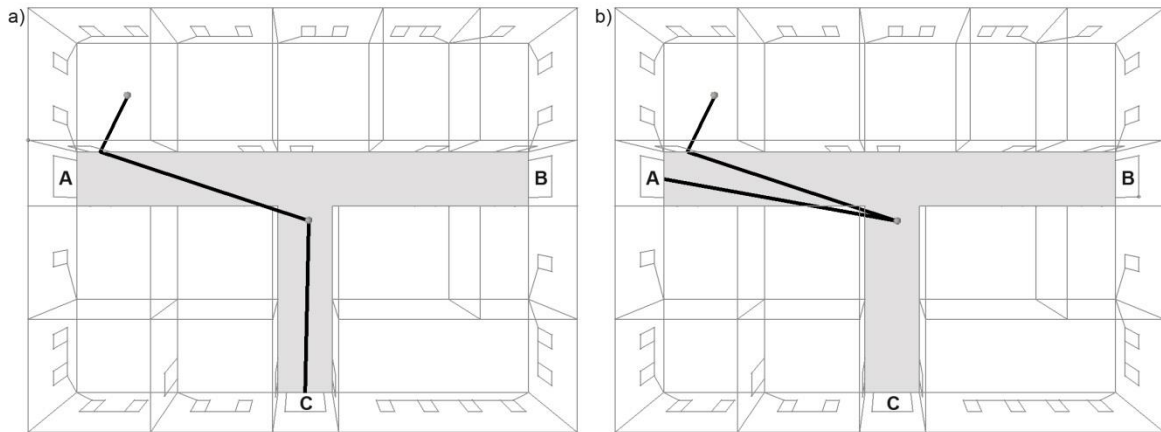
176 Figure 2a illustrates a close-up of a single level, the ground floor, in the building shown in Figure 1.  
 177 The corridor (the grey area) is connected to adjacent rooms by doors and to the outdoors by exits A-

178 C; there are three staircases S1-S3. The logical network representing connections among rooms at  
179 the ground floor is shown in Figure 2b. Other vertical connections between adjacent rooms at  
180 different levels are also included in the logical network (see Figure 1c). In a non-emergency scenario,  
181 only standard navigation routes via doors are used. These routes are represented by a sub-network  
182 of the logical network shown in Figure 2c.



185 Figure 2. Ground floor of the building represented with the DHE: a) grey area represents a corridor  
186 with three exits A-C; S1-S3 are staircases; b) logical network; c) sub-network reflecting navigable  
187 connections through doors.

188 The network can be effectively used for navigation routes in simple models, e.g. when it consists of  
189 'cubical' rooms with one door or two doors located on opposite walls. A problem arises when rooms  
190 have a complex shape and many doors (e.g. long corridors, concave rooms, big open spaces). If the  
191 shortest path from a room to the closest exit goes through a corridor node, located in the geometric  
192 centre, an incorrect exit may be selected (see Figure 3a). In reality, the shortest path between the  
193 graph nodes is calculated properly, but navigation routes within a corridor are not represented  
194 correctly. In addition, if the path finding algorithm is forced to select the correct closest exit (A in  
195 Figure 3b), then the path is not a 'natural' way of navigation – no one goes to the centre of a  
196 corridor first and then takes the correct door. A solution to the problem is to enhance the model by  
197 providing a better representation of 'natural' ways of indoor navigation.



198

199 Figure 3. Paths (black lines) from a selected room through the corridor (grey area) to one of the exits  
 200 (A-C are exits from a building): a) C is wrongly calculated as the closest exit; b) A is the closest exit  
 201 but the path is not a 'natural' way of navigation.

202 The closest model is the one proposed by Liu and Zlatanova (2012), where the logical network  
 203 representing a building structure is combined with navigable networks within single rooms: the  
 204 network generation algorithm is based on the location of doors and concave corners. However, the  
 205 navigable network is built from a spatial subdivision, the Voronoi tessellation, which is related to the  
 206 method proposed by Lee (2004).

207 In this paper, a novel approach of navigable network generation, the Variable Density Network  
 208 (VDN), based on the Voronoi Diagram is proposed. This approach allows a new automated method  
 209 for deriving a navigable network in a 3D indoor environment, including a full 3D topological model,  
 210 which may be used not only for standard navigation but also for finding alternative egress routes  
 211 and simulating phenomena associated with disasters such as fire spread and heat transfer. The main  
 212 application for the proposed network is calculation of egress paths in a dangerous environment to  
 213 assist rescue teams, thus, evacuation of people and related topics, such as determination of  
 214 position, route tracking, crowd simulation, human and social behaviour, are not taken into  
 215 consideration. This can be a part of a bigger emergency response system.

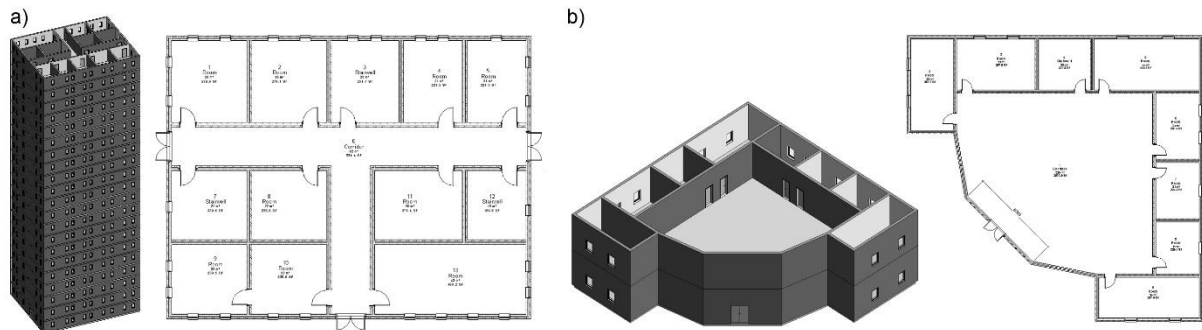
216 ~~The main focus of this research is a decision support system to assist emergency teams to determine~~  
 217 ~~egress paths in the event of emergency, thus, evacuation of people and related topics, such as crowd~~  
 218 ~~simulation, human and social behaviour, are not taken into consideration.~~

### 219 **3.2. Methodology**

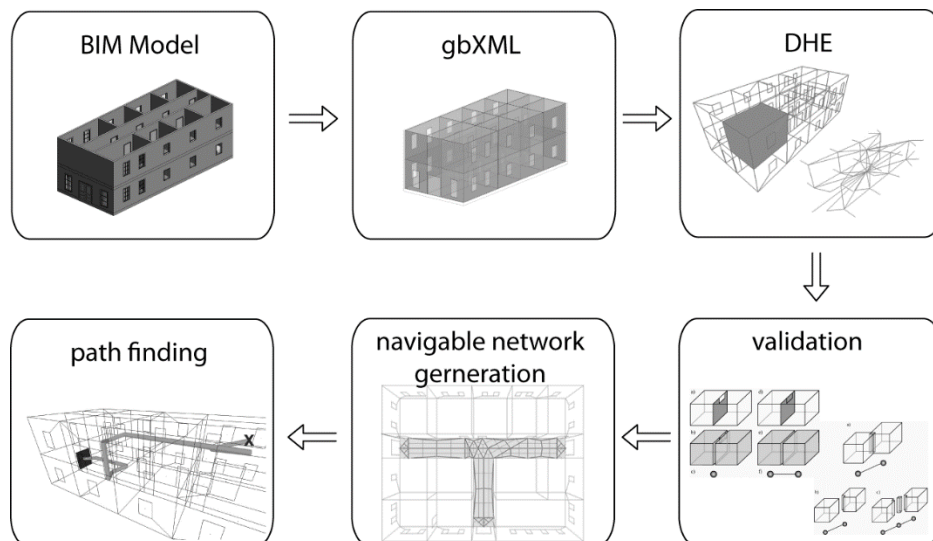
220 In this research, two mock data models and a real-life case study were created in order to illustrate  
 221 the proposed new method of navigable network generation (VDN). The first model is a high-rise  
 222 office building with cubical rooms connected to a centrally located corridor (see Figure 4a). It is used  
 223 to illustrate how the method works in narrow corridors of a complex shape with several doors to  
 224 adjacent rooms. The second model is a two-storey building with a central big open space (see Figure  
 225 4b). It is used to show applicability of the same method to open spaces. The third model represents  
 226 a floor plan of the Doha World Trade Centre in Qatar. This model is selected to carry out a  
 227 comparative study between the proposed VDN and other prevailing models. The models were built  
 228 in the Autodesk Revit design environment and exported to the gbXML data format. A gbXML file was  
 229 imported and analysed in in-house software developed for testing purposes. Models are



230 represented using the DHE data structure, which is an integral part of the in-house system. Some  
 231 models may require validation in order to preserve a consistency between geometry and topology,  
 232 which in particular concerns detection and fixing two problems: missing faces and overlapping  
 233 between adjacent rooms. The workflow is shown in Figure 5.



234  
 235 Figure 4. Mock data models – 3D views and ground floor plans: a) high-rise building; b) two-storey  
 236 building.



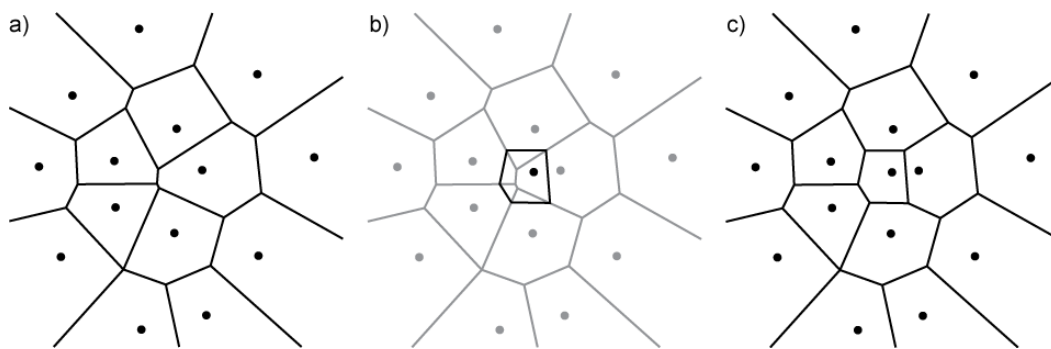
237  
 238 Figure 5. Method workflow.

239 The model enhancement, proposed in this paper, introduces a novel network for indoor navigation  
 240 in spaces along navigation routes, such as corridors, big open spaces, rooms with several doors. A  
 241 floor is tessellated using a VD construction algorithm, where doors and concave corners are initial  
 242 Voronoi vertices (nucleation points), and additional points are added in order to create a denser  
 243 tessellation. The nucleation points from adjacent cells are connected by links, thus forming a  
 244 network, which is better suited for navigation, than the network without such innovation.

245 There are several advantages to this strategy: 1) path finding algorithms for the additional network  
 246 give more accurate results within a single room; 2) the additional network is generated using a 2D  
 247 algorithm and does not affect the original network representing the 3D topology of a building; 3)  
 248 the same method may be applied for corridors and big open spaces of an arbitrary shape; 4) 'natural'  
 249 paths for human movement are reflected in the network.

250 The proposed method consists of several steps: A) spaces (we will call them rooms in the following  
 251 description) with more than one door are selected; B) the floor of the selected room is detected  
 252 based on semantic information from the original BIM model or, if this information is not available,  
 253 then surfaces with the normal vector pointing upwards are considered as a floor; C) dual nodes  
 254 representing doors are projected on the floor and together with concave vertices of the floor surface  
 255 are selected as nucleation points for a tessellation algorithm – they are called ‘constraint nucleation  
 256 points’ in the following description; D) the VD algorithm is performed iteratively and additional  
 257 points are added; the nucleation points of neighbour cells are connected by links forming a network;  
 258 E) the locations of additional nucleation points occurring on constraint edges are moved towards the  
 259 geometric centre of the associated cell, while the original location of the constraint points is not  
 260 changed.

261 The process of the VD construction (see Step D above) requires a detailed description. An iterative  
 262 algorithm for the constraint VD was implemented based on the Green and Sibson algorithm (Green  
 263 and Sibson, 1978), see Figure 6.



264

265 Figure 6. Process of Voronoi Diagram construction: a) existing tessellation; b) new vertex and its  
 266 Voronoi cell; c) tessellation after point insertion.

267 The floor is represented by a polygon of an arbitrary shape. The original polygon edges are  
 268 constraint edges, which are not modified in the tessellation process. In the first iteration dual nodes  
 269 representing doors, projected on the floor and concave corners, are selected as constraint  
 270 nucleation points. The locations of the constraint points are not changed later. The nucleation point  
 271 is always enclosed by a single Voronoi cell. Subsequently, each node is connected by links with nodes  
 272 from adjacent cells; all these links and nodes form a network. In the next step, new nucleation points  
 273 are added at the middle of each link if the link is bounded by constraint points, or if both bounding  
 274 points lie on constraint edges, which are not co-linear. The process is repeated until no new points  
 275 may be added because they would be too close, or a certain number of iterations have been  
 276 reached.

277 An algorithm for VD construction is presented below as Algorithm 1. In the examples presented in  
 278 this paper, the following input parameters were used: the threshold  $T_1=6$  (see Figure 7c and Figure  
 279 8b), the threshold  $T_2=0.7$  (see Figure 9) and the maximum tessellation level  $TL_{max}=10$ .  $T_2$  is used if an  
 280 edge  $e$  in the tessellation is close to the hazard location. In this paper,  $e$  is considered to be close to  
 281 the hazard location if  $length(e) \times 3 > distance(u, h) + distance(v, h)$ , where:  $u$  and  $v$  are end-points of  $e$   
 282 and  $h$  is the hazard location.

283 For the sake of algorithm clarity, only one polygon representing a floor is considered. If a floor is  
284 represented as a set of adjacent polygons in an original model, they may be merged into one and the  
285 same algorithm can be used.

286 **Algorithm 1:** Navigable network generation (tessellation of a floor)

---

287 **Input:** The cell representing room  $R$ .

288 The floor polygon for  $R$ .

289  $T_1, T_2$  (threshold values for edge length).

290 Maximum tessellation level  $TL_{max}$

291 **Output:** Tessellation  $f$ .

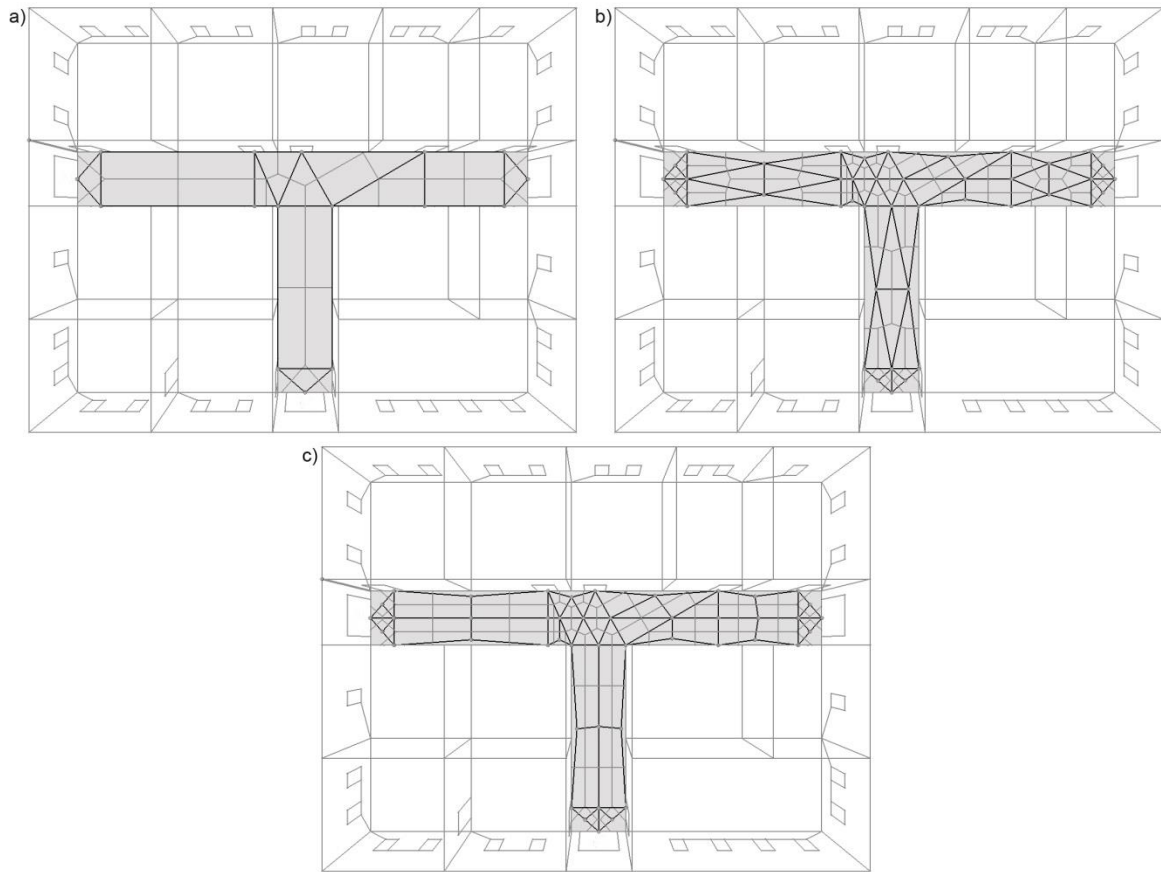
- 292 1. Make a copy of the floor polygon, denoted by  $f$ .
- 293 2. Calculate the number of doors in room  $R$ , denoted by  $d$ . If  $d \leq 1$ , then stop the algorithm (no  
294 network generation is necessary).
- 295 3. For each door dual node, make its projection on the boundary of  $f$ .
- 296 4. Create a list  $N$  consisting of constraint nucleation points for VD in order of their appearance on  
297 the boundary of  $f$ . The constraint nucleation points are door nodes and concave corner nodes.  
298  $f$ .
- 299 5. Create a list  $V$  of VD cells and put  $V_1=f$ . (The floor polygon  $f$  is the initial Voronoi cell associated  
300 with  $N_1$ .)
- 301 6. Put  $TL=1$ , where  $TL$  is the current tessellation level.
- 302 7. Take the first unprocessed element from  $N$ , denoted by  $N_j$ .
- 303 8. Create a list of cells for testing, denoted by  $CT$  and add to it a cell from  $V$ , which includes node  $N_j$
- 304 9. Take the first unprocessed element from  $ctest$  and denote it by  $V_k$  (it is associated with  $N_k$ ).
- 305 10. Calculate a bisector line  $bi$  of the segment  $(N_j, N_k)$ .
- 306 11. Calculate intersection points of  $bi$  with  $V_k$ . The set of such points is denoted by  $IP$ .
- 307 12. If the number of points in  $IP$  is greater than 2, then do the following:
  - 308 a. In  $I$  find two intersection points whose line segment divides the cell  $V_k$  into two parts such that  
309 each part includes one of the nodes  $N_j$  and  $N_k$ ;
  - 310 b. Remove the rest of the intersection points from  $IP$ .
- 311 13. If the number of points in  $IP$  is less than 2, then go to Step 9.
- 312 14. Create the edge  $(j,k)$  bounded by intersection points from  $IP$ , and insert it into the existing  
313 tessellation of the polygon  $f$ . The edge  $(j,k)$  divides  $V_k$  into two cells:  $C_j$  and  $C_k$  such that  $N_j$  is located  
314 in  $C_j$  and  $N_k$  in  $C_k$ .
- 315 15. Add  $C_j$  to  $V$ , i.e.  $V_j=C_j$ , and put  $V_k=C_k$ . (The edge  $(j,k)$  is a part of the boundary of the newly created  
316 cell for  $N_j$ .)
- 317 16. Add those cells to the list  $CT$ , which are adjacent to the edges intersected by the edge  $(j,k)$ , taking  
318 into account the following:
  - 319 a. If an intersected edge is a constraint edge (the initial boundary of  $f$ ), then add all cells adjacent  
320 to  $V_k$ .
  - 321 b. If a cell is already in  $CT$ , then do not add it.
- 322 17. If there are unprocessed elements in  $CT$ , then go to Step 9. (Otherwise the boundary of the new  
323 cell for  $N_j$  was created.)

- 324 **18.** Remove all edges from inside the boundary of the newly created cell for  $N_j$ . (This is illustrated in  
 325 Figure 6, the transition from b) to c).)
- 326 **19.** If there are unprocessed elements in  $N$ , then go to Step 7. (Otherwise the current level of  
 327 tessellation is completed.)
- 328 **20.** If  $TL < TL_{max}$ , then for each edge  $e$  connecting nucleation points of adjacent cells in  $vd$ , do the  
 329 following. Calculate the bisector point  $B$  for  $e$  only if:
- 330 **a.**  $e$  is longer than  $T_1$ ; or  
 331 **b.**  $e$  is close to the hazard location and it is longer than  $T_2$ ; or  
 332 **c.**  $e$  is bounded by two constraint nucleation points (doors or concave corners); or  
 333 **d.** both end-points of  $e$  lie on constraint edges, which are not co-linear.
- 334 Add the point  $B$  into  $N$ .
- 335 **21.** If  $TL < TL_{max}$  and there are unprocessed elements in  $N$ , then  $TL=TL+1$  and go to Step 7.
- 336 **22.** If there are nucleation points in  $np$ , other than constraint nucleation points, which are located on  
 337 constraint edges (the initial boundary of  $f$ ), then move locations of those points towards the  
 338 centre of the associated cells.
- 339 **23.** Report  $f$ . Algorithm stops.

---

341 The first iteration of the tessellation (grey cells) and the corresponding network (black edges) are  
 342 shown in Figure 7a. Because the tessellation is not dense, the network consists of few links. Many of  
 343 them lie on constraint floor edges. Therefore, several navigation routes go from door to door along  
 344 walls. The process stops after the second iteration generates shorter links (see Figure 7b). Shorter  
 345 links are the result of new point insertion in the midpoint of the original link, which leads into  
 346 generation of a Voronoi cell with associated dual edges (i.e. shorter links) connecting the new cell  
 347 with neighbour cells. The locations of new nucleation points occurring on constraint edges are  
 348 modified by moving them towards the centre of the associated cell (see Step E), which overcomes  
 349 the problem of navigation along walls. However, there are some links in the network, which are  
 350 perpendicular to the walls, and their bounding points occur on constraint edges. Such links may  
 351 produce sharp turns on navigation routes. Additional nodes and links are added in the next  
 352 iterations, which solves this problem. The final result is shown in Figure 7c. The tessellation and  
 353 corresponding network are attached to the dual node representing the room. The network is used  
 354 for precise path calculation within a room.

355

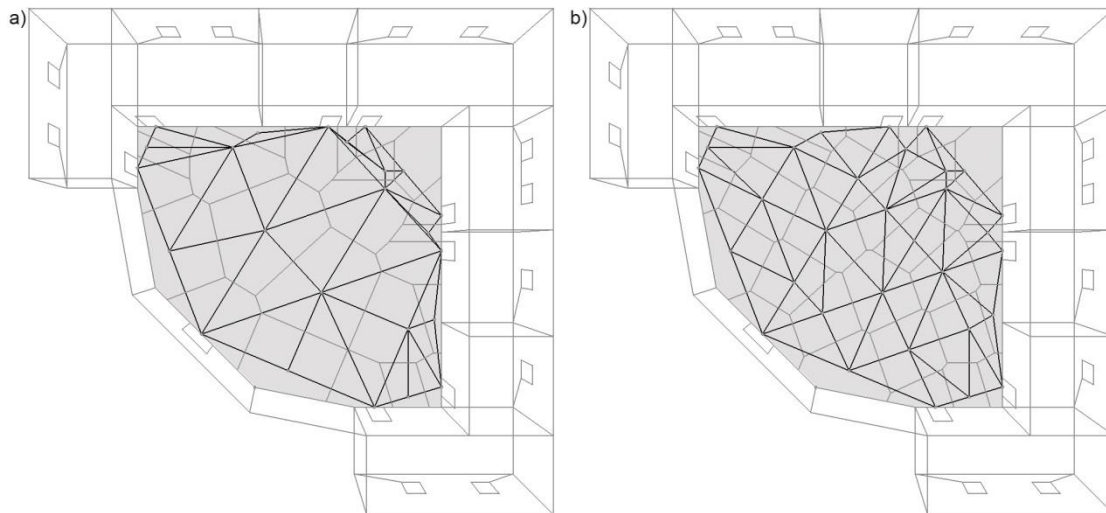


356

357 Figure 7. Floor tessellation (grey cells) and associated network (black lines): a) first iteration; b)  
358 second iteration; c) final tessellation.

359 An advantage of the proposed solution is that it can be applied not only to corridors but also to any  
360 room shape, e.g. irregular spaces. This is an important property, which helps to avoid the need to  
361 classifying a room as a corridor or an open space, and then performing different algorithms for  
362 network generation. An example of an indefinable area is a narrow corridor which, at some point,  
363 turns into a bigger area (a hub) with many doors or a junction with other corridors.

364 However, in this scenario, long links in the network may be introduced, because nucleation points in  
365 the central area of a room are enclosed by relatively bigger cells and the distance to neighbours is  
366 bigger (see Figure 8). This may produce 'wobbling' paths. Consequently, for links that are longer than  
367 a specified threshold, new nucleation points are introduced in the midpoint of these links.

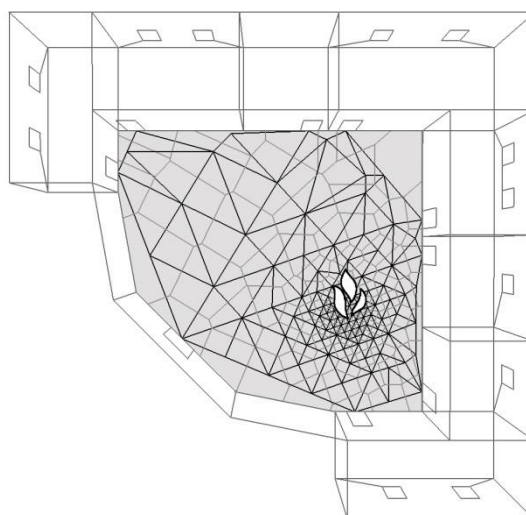


368

369 Figure 8. Tessellation of big open space (grey area): a) tessellation without a maximum link length  
 370 threshold; b) tessellation with a maximum link length threshold (in this case 6 m).

371 The higher density of the network is helpful for finding alternative or safest paths when a hazardous  
 372 event takes place within an open space: some nodes may be prohibited for navigation, while the rest  
 373 of the space, with a lower risk, is still considered as safe. This applies to buildings such as airports or  
 374 shopping malls.

375 The network might be densified around a dangerous area using the same method. For links located  
 376 closer to the hazard source, a smaller threshold for links is introduced. Therefore, new nucleation  
 377 points are introduced in the midpoints of these links and new shorter links are introduced. This  
 378 operation provides local network densification (see Figure 9). TODO: (move to introduction???)  
 379 Densification is commonly applied in the finite element mesh generation and refinement (Du and  
 380 Gunzburger, 2002; Ho-Le, 1988; Petersen and Martins, 1997).



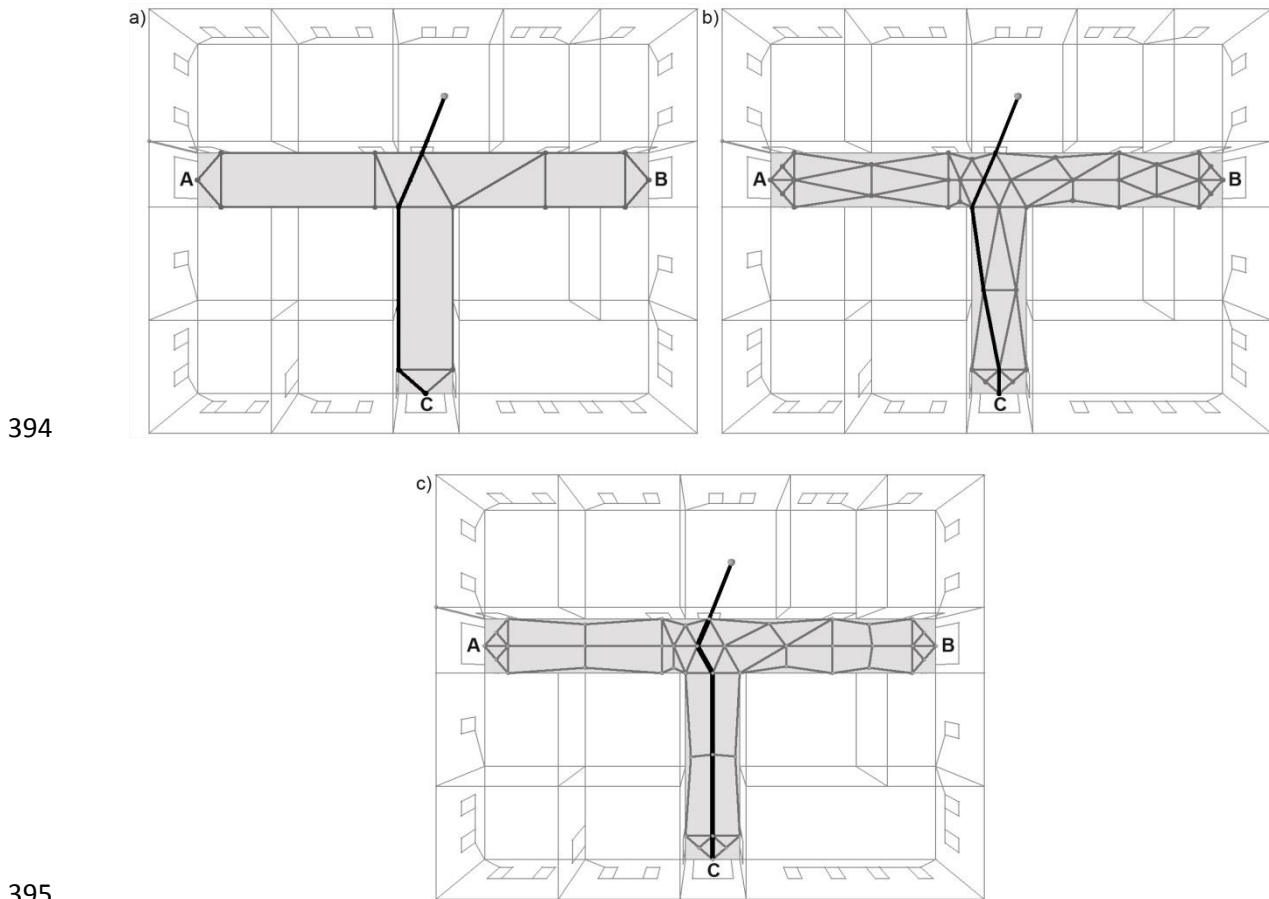
381

382 Figure 9. Local densification of the navigable network around a hazardous area.

### 383 **4.3. Results and discussion**

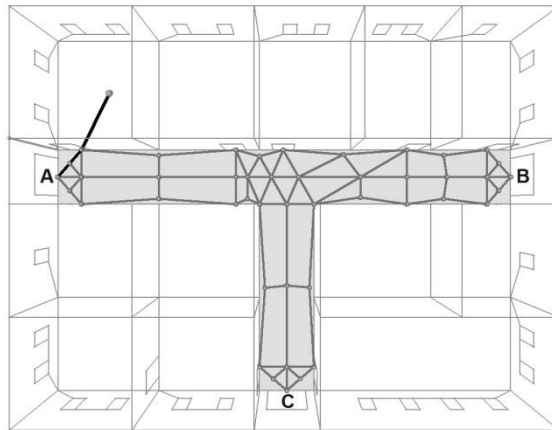
384 The main reason for introducing additional nucleation points is to improve the network for a path  
 385 finding application. This increases the number of cells in the tessellation, thus the number of

386 network links is increased and they are shorter. If the tessellation process is finished after the first  
387 iteration, a path between two locations goes through constraint points, which is not a 'natural' route  
388 for navigation – it is like walking from door to door along walls (see Figure 10a). The second iteration  
389 produces a network better suited for navigation, but the path is slightly 'wobbling' (see Figure 10b),  
390 mainly because there are links that cross the corridor – perpendicular to the constraint edges. The  
391 path based on the final network is still influenced by 'wobbling' but less than in the previous  
392 iterations (see Figure 10c), and it is acceptable in the presented research, since a very precise path  
393 calculation is not required.



396 Figure 10. Shortest path from a selected room to door C: a) using the network produced by the first  
397 iteration; b) using the network produced by the second iteration; c) using the final network.

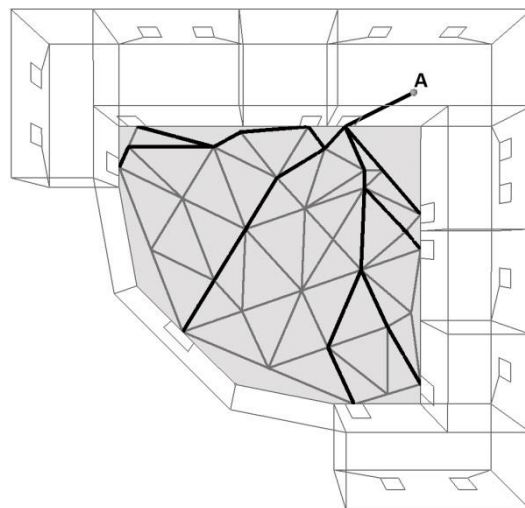
398 The proposed method solves the problem of incorrect paths shown in Figure 3. When the additional  
399 network within the corridor is used, the result of the shortest path finding algorithm is correct (see  
400 Figure 11). The egress route from the selected room goes through the door straight to the nearby  
401 exit.



402

403 Figure 11. The shortest path from a selected room to exit A (A-C are exits from a building) based on  
 404 the original network and the network produced by the corridor floor tessellation.

405 A satisfactory improvement is also achieved in the case of open spaces. All shortest paths from a  
 406 selected room to all doors of the open space are shown in Figure 12. The network within the room is  
 407 a better approximation of 'natural' navigation routes than the original logical network.



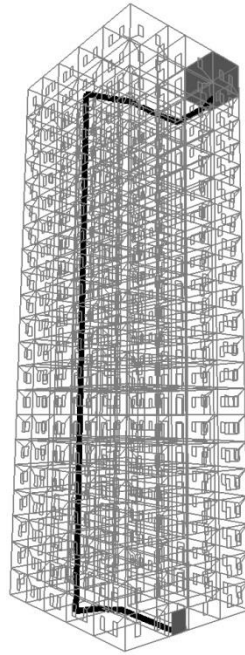
408

409 Figure 12. Shortest paths (black lines) from a selected room (A) to all doors of an open space.

410 The result of Dijkstra's algorithm applied from a selected room in the building is shown in Figure 13.  
 411 The shortest path goes from the room at the top floor to the ground floor through one of three  
 412 staircases located near the room. All corridors and rooms with more than one door in the building  
 413 were automatically tessellated and the navigable network was retrieved before the application of  
 414 the path finding algorithm.

415 It should be noted that the building model used here is a mock dataset, where the main navigation  
 416 routes include corridors and staircases, and lifts are not included in the model. However, lift shafts  
 417 may be considered for navigation in the same way as staircases but normally they cannot be used in  
 418 case of emergency situations.





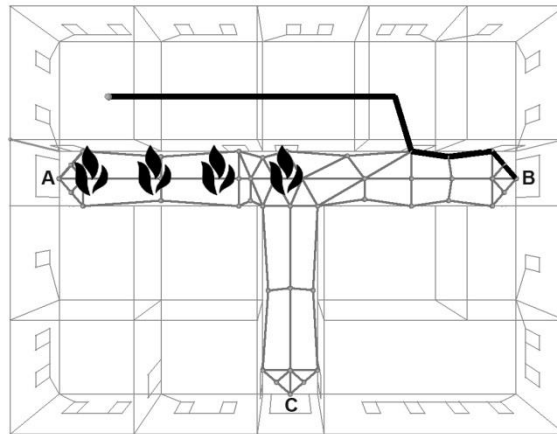
419

420 Figure 13. Egress route (black lines) from a selected room (grey cell) to the closest exit (grey door).

421 The logical network may be used for alternative path finding in the case of an emergency, when the  
422 conventional navigation routes are blocked. In the hypothetical scenario shown in Figure 14, a  
423 section of the corridor may be on fire. Therefore, it is not safe to use a conventional route to leave  
424 the selected room and reach exit A as a result of a fire behind the door. Thus, an alternative path is  
425 calculated, which goes through walls, where a hole can be possibly made. Once the room with a  
426 door located outside the dangerous area is reached, a conventional egress route to exit B is used.

427 Alternative paths are found automatically if there is no safe connection from a room through doors.  
428 A connection from the logical network with the smallest weight is selected. The weight for each wall  
429 in the room may differ depending on a construction material. Therefore, walls easier to demolish are  
430 selected as candidates for navigation, e.g. partitions made of plaster panels is favoured over walls  
431 made of concrete.

432 It is important to note that windows may be considered as alternative exits if they are located close  
433 above the external ground, for example, windows on the ground floor. In addition, rescue teams are  
434 able to get inside the building through windows located high above the ground using ladders. In  
435 order to show navigation through walls using the logical network windows were not allowed to be  
436 used in the illustrated simulation.



437

438

Figure 14. Alternative path finding.

439

Another type of alternative paths are the safest paths, which avoid dangerous areas using normal navigation ways. Typically they are longer than shortest paths but they are located as far from hazard as possible. In current research, an abstract hazard is manually triggered in selected rooms and is propagated within a building. If information from sensors (e.g. temperature and smoke sensors) is available, a hazardous event may be automatically detected. In hazard simulation, additional weights reflecting hazard spread in the network are calculated based on the number of obstacles, such as walls, and distance from hazard locations. Then, new safest paths are calculated using these new weights.

446

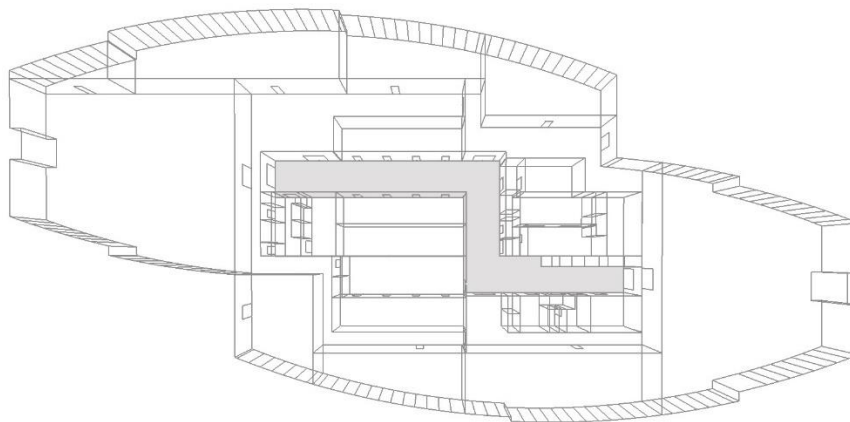
447

#### 5.4. Comparison of VDN with prevailing indoor navigable networks

448

Two state of the art methods of the navigable network reconstruction used in emergency response research (Lee, 2004; Liu and Zlatanova, 2011) were selected for a comparison. The reason for this selection is the close relationships to the VDN method proposed in this paper. Three configurations of rooms shown in Figure 7, Figure 8 and Figure 15 are used as examples for this comparison: T-shaped corridor (also see Figure 16 a), d), g) and j)), open space (also see Figure 16 b), e), h) and k)) and Z-shaped corridor (also see Figure 16 c), f), i) and l)), respectively. Two first examples are mock data, while the latter is a real building – World Trade Centre in Doha, Qatar.

454



455

456

Figure 15. Floor plan – World Trade Centre in Doha, Qatar. Grey-shaded corridor is used for comparison with other methods.

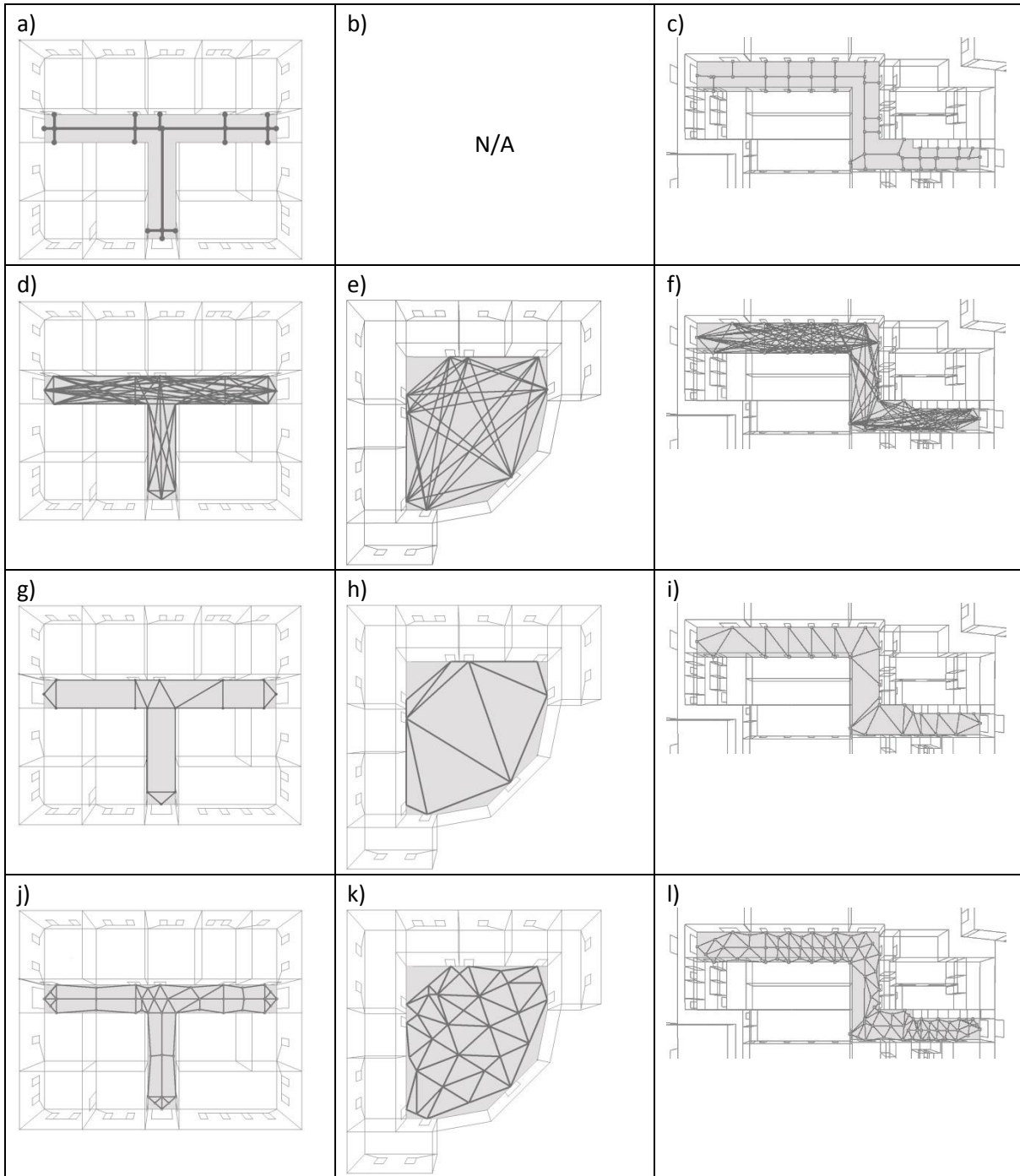
457

458 Lee (2004) proposed the Node-Relation Structure (NRS) as the topological model. The Straight  
459 Medial Axis Transformation is applied for generating a navigable network within a corridor. A  
460 skeleton of the corridor floor is calculated; this is based on VD construction. The result is a linear  
461 representation of a polygon – a ‘backbone’ representing a navigation route through the corridor.  
462 Nodes representing rooms adjacent to the corridor with a door in between are connected to the  
463 skeleton by additional links. The advantage of this method is that it is a simple network with a  
464 relatively small number of links (see Table 1).

465 However, the applicability to big open spaces was not presented, possibly because of unsatisfactory  
466 representation of navigation routes. Consequently, it is suggested that it is not practical to use the  
467 aforementioned method for spaces other than simple-shaped corridors. Additionally, because the  
468 skeleton is located in the middle of the corridor and the adjacent rooms are connected to the  
469 skeleton by perpendicular links, the network does not reflect ‘natural’ ways of navigation – if two  
470 doors are coplanar, i.e. located on the same wall, one must go from the first door to the middle of a  
471 corridor, turn 90 degrees, walk in the middle of the corridor towards the second door, turn 90  
472 degrees again, and then get to the second door. This may be not a significant drawback, especially  
473 for narrow corridors when the shortest paths are calculated. However, as complexity increases, it  
474 may become significant in computation of the simplest paths, where the sharpness of turn angle  
475 is considered.

476 The door-to-door (DtD) method (Liu and Zlatanova, 2011) is based on a simple idea of navigation  
477 from a selected door directly to another door, if two doors are in direct visibility. If there is no direct  
478 visibility, then intermediate concave corridor corners are introduced to the path. Taking all possible  
479 connections among all the doors within a corridor including concave corners, the navigable network  
480 consists of more links than NRS (see Table 1). The network is a non-planar graph in the considered  
481 examples. The method may be easily applied for big irregular spaces.

482 These two methods produce a fixed network depending on the geometry of a room and location of  
483 doors. This may be a drawback when alternative paths within a big room are necessary to calculate,  
484 for instance to avoid hazard located in the room. This is critical, when big open spaces in a shopping  
485 mall or airport are considered. In contrast, the proposed VDN method is more flexible, mainly  
486 because the density of tessellation may be easily increased resulting in more links in the network  
487 and thus more flexible routes (see Table 1).



488 Figure 16. Navigable networks generated for different floor shapes using different methods: a)-c)  
489 NRS; d)-f) DtD; g)-i) VDN (1<sup>st</sup> level); j)-l) VDN (max. level with the threshold).

490 It should be noted, that the number of links calculated for the DtD method is based on the following  
491 assumption: links connecting the same nodes are not duplicated in the network. For example,  
492 considering three doors  $d_1$ - $d_3$  and one concave corner  $c_1$ , if doors  $d_1$  and  $d_2$  are in a direct visibility  
493 and  $d_3$  is connected with  $d_1$  and  $d_2$  through  $c_1$ , there are four links:  $d_1$ - $d_2$ ,  $d_1$ - $c_1$ ,  $d_2$ - $c_1$  and  $c_1$ - $d_3$ .

494 It should be also noted that, in the NRS construction, the skeleton of the corridor is calculated based  
495 on straight medial axis transformation. Door nodes are connected to the skeleton by line segments,  
496 which are perpendicular to the skeleton, and new nodes at an intersection point are added to the  
497 skeleton. However, if the distance from a door to an existing node in the skeleton is shorter than the

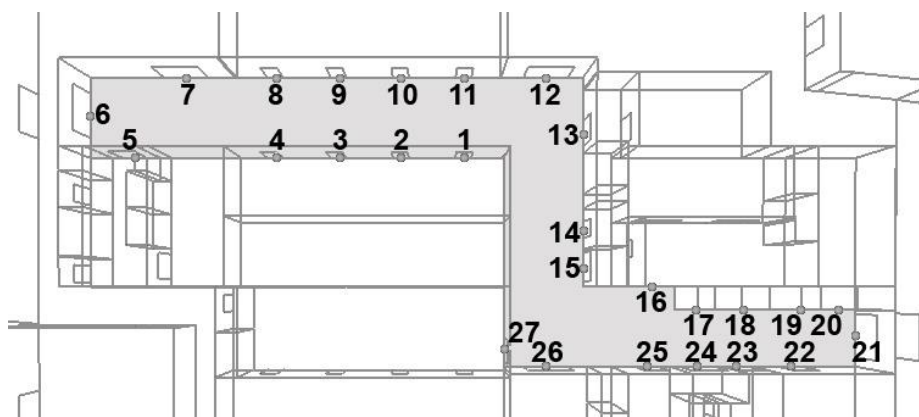
498 perpendicular connection, the door node is connected to that node. Conversely, in order to avoid  
 499 very short links in the network, a door node is connected to an existing node if a new intersection  
 500 point is located within a range of 10 cm from the existing node.

501 Table 1. Number of nodes and links in navigable networks generated using different methods.

	<b>NRS (Lee, 2004)</b>	<b>DtD (Liu and Zlatanova, 2011)</b>	<b>VDN (1<sup>st</sup> level)</b>	<b>VDN (max. level with the threshold)</b>
<b>T-shaped corridor</b>	20 nodes 20 links	16 nodes 77 links	16 nodes 26 links	45 nodes 84 links
<b>Open space</b>	N/A	9 nodes 36 links	9 nodes 15 links	32 nodes 74 links
<b>Z-shaped corridor</b>	47 nodes 46 links	30 nodes 187 links	30 nodes 56 links	85 nodes 190 links
<b>Comments</b>	- simple network with a small number of links - limited applicability to open spaces	- non-planar graph - minimized number of links on door-to-door routes	- variable number of links depending on densification level - local network densification possible	

502

503 In order to compare the precision of different methods for tessellation, we consider the main  
 504 corridor of the actual floor plan of the Doha World Trade Centre (see Figure 15). There are 27 doors  
 505 in the corridor as depicted in Figure 17. Ten pairs of doors were randomly generated, which  
 506 represent ten random possibilities for moving from one door to another in the corridor (see Table 2).  
 507 For each pair of doors, the length of the actual walking path between them was calculated, as well as  
 508 the lengths of paths generated by the NRS method, the DtD approach and the VDN method for the  
 509 first and maximal levels of tessellation. The corresponding results are summarised in Table 2.  
 510 Examples of path  $P_6$  generated by the aforementioned methods are shown in Figure 18.



511

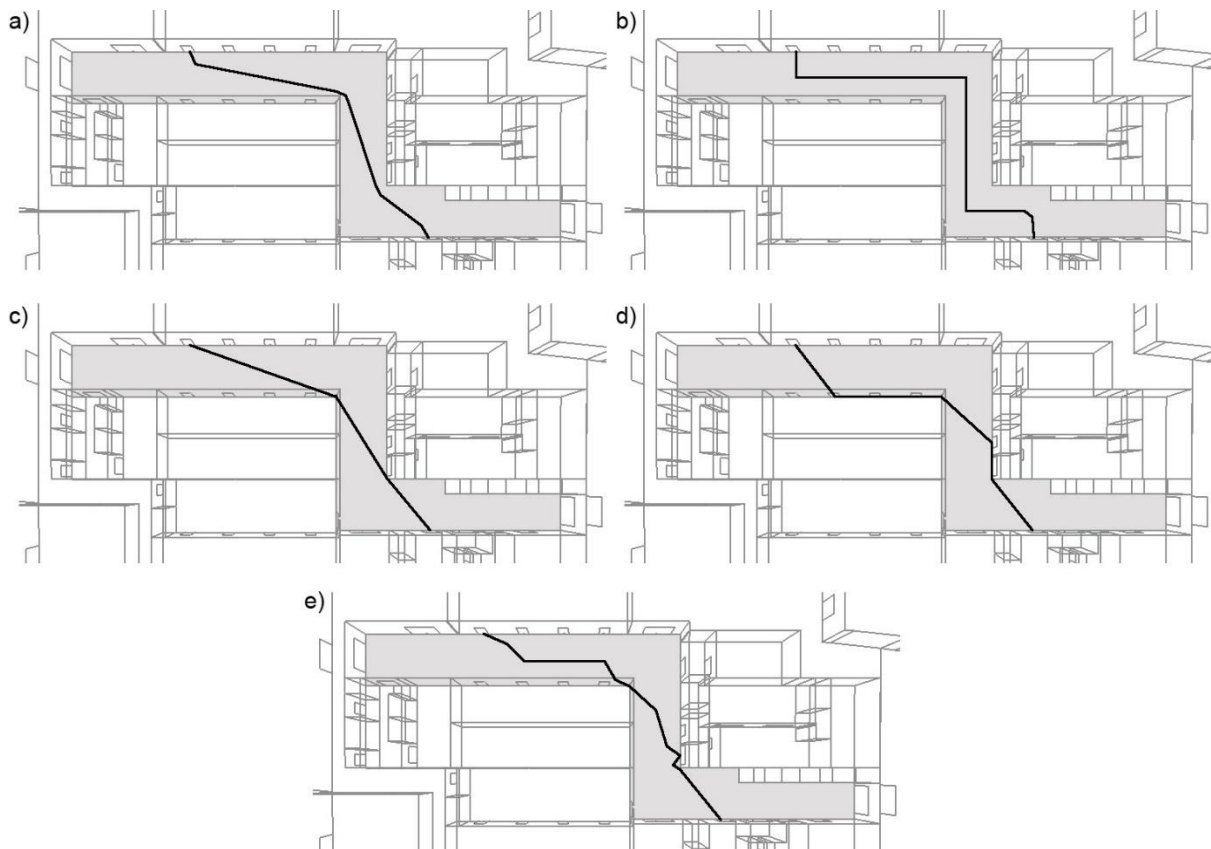
512

Figure 17. Location of doors 1-27.

513 Table 2. Ten random routes and their lengths (meters) for different methods

Path	From Room	To Room	Actual Route	NRS	DtD	VDN (1 <sup>st</sup> level)	VDN (max level with the threshold)
$P_1$	11	23	18.8	24.1	18.0	19.3	19.5
$P_2$	7	9	7.4	10.1	6.6	6.6	6.8
$P_3$	5	16	28.1	34.3	25.4	26.0	27.3
$P_4$	17	12	15.7	18.8	14.1	14.8	16.1
$P_5$	15	20	14.1	18.1	12.0	12.2	13.2
$P_6$	25	8	22.7	28.3	21.4	23.1	23.1
$P_7$	10	26	15.7	18.7	14.8	17.1	15.6
$P_8$	20	18	5.1	6.2	4.1	4.1	4.2
$P_9$	9	1	6.8	8.9	6.4	7.1	6.6
$P_{10}$	22	2	22.9	29.0	20.6	22.0	22.6

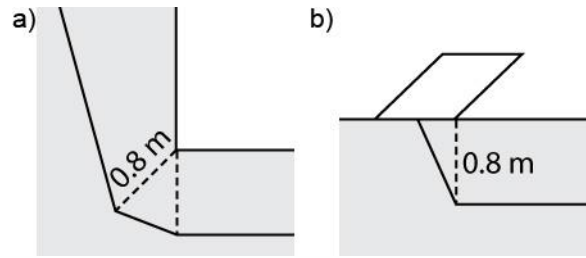
514



515

516 Figure 18. Path  $P_6$  from room 25 to 8 generated by methods: a) actual walking path; b) NRS; c) DtD;  
 517 d) VDN (1<sup>st</sup> level); e) VDN (max level with the threshold)

518 The actual path, which is a point of reference in this comparison, was generated manually  
 519 considering the following rules: the path should not run closer than 0.8 m to the concave corners  
 520 (see Figure 19a); a next node after a door node is located 0.8 m from the door frame into direction  
 521 of the next move (see Figure 19b); the direction of door opening is not taken into consideration.



522

523 Figure 19. Actual path generation: a) distance from a wall; b) distance from a door.

524 Furthermore, three standard errors were calculated: the mean error (ME), the mean absolute error  
 525 (MAE) and the mean squared error (MSE). Note that the former represents the bias, whereas the  
 526 last two refer to the accuracy of methods. The results are given in Table 3. The NRS method very  
 527 often overestimates the length of the actual path, which is reflected in the ME equal to -3.9m,  
 528 whereas the DtD approach tends to underestimate the length with ME=1.4 m. On average, there is  
 529 some underestimation in the VDN method with the ME=0.5 m and 0.2 m for the first and maximal  
 530 levels. The MAE figures for the above methods are similar: 3.9 m, 1.4 m, 1.0 m and 0.5 m,  
 531 respectively. The same numbers expressed as percentages of the MAE to the average length (15.7  
 532 m) of actual routes are as follows: 24.8%, 8.8%, 6.4% and 3.3%, thus the 5% standard threshold for  
 533 errors is achieved by the maximal level of tessellation in the VDN method. Finally, the MSE measure,  
 534 which penalises large errors, is rather high (18.1) for the NRS method, whereas the DtD and VDN  
 535 approaches exhibit small MSEs as can be seen in Table 3. Thus, the VDN method with the maximal  
 536 level of tessellation demonstrates the best characteristics for the bias and accuracy.

537 Table 3. Errors of the four methods

	NRS	DtD	VDN (1st level)	VDN (max level)
<b>ME</b>	-3.9	1.4	0.5	0.2
<b>MAE</b>	3.9	1.4	1.0	0.5
<b>MSE</b>	18.1	2.4	1.3	0.4

538 **6.5. Conclusions**

539 In this paper, the navigable indoor network reconstruction from an indoor model was presented and  
 540 compared with other methods [applied for route planning](#) in the field of emergency preparedness  
 541 and response. The network consists of a logical network reflecting the 3D building structure and a  
 542 detailed navigable network within rooms with many doors and complex geometry. The logical  
 543 network represents the full 3D topology including spatial relations between rooms at different floors  
 544 and rooms sharing a wall without doors or other openings. It can be used not only for indoor  
 545 navigation but also for alternative path finding and potential simulations of various phenomena  
 546 associated with emergency situations.

547 DHE data structure was used in this research to represent a 3D indoor scene reconstructed from a  
 548 BIM model. Two graphs, primal and dual, stored and updated simultaneously allow for the  
 549 geometry, topology and semantics representation in one consistent model. They are used for direct  
 550 implementation of Dijkstra's algorithm for path-finding and visualisation of the model, and egress  
 551 routes.

552 To demonstrate the robustness of the VDN approach, a static model was presented. This consists of  
553 a structure of the building and location of events that are known before the navigable network is  
554 generated. In case of a new event, the whole navigable network within an affected room is  
555 generated from the start. However, local densification of the network may be performed, when  
556 necessary, without recalculating the whole network.

557 The VDN algorithm may be applied to any space type including corridors and big open spaces, unlike  
558 other methods, which focus on corridors only. The tessellation may be easily densified locally or  
559 within the whole space by changing the threshold for a link length, which increases the number of  
560 links in the navigable network. This may be helpful in finding alternative paths within a single big  
561 room with a hazardous event located within the room. Because VDN is generated independently for  
562 each space, a different tessellation level and threshold may be defined for different spaces, for  
563 example, denser network available within corridors, while sparse in rooms.

564 It was shown that VDN, in comparison to prevailing approaches, increases accuracy of egress route  
565 planning. The length of paths calculated using VDN is closer to the length of 'natural' paths taken by  
566 pedestrians. Comparison study was performed in a model of the real building: Doha World Trade  
567 Centre in Qatar.

568 The proposed method uses basic algorithms for network construction (Green and Sibson algorithm  
569 for VD generation), densification (new nucleation points added in the middle of links longer than a  
570 threshold) and path-finding (Dijkstra's algorithm) in order to present a general idea and its  
571 applicability in emergency response applications. It may be improved by using advanced algorithms  
572 for better Voronoi point location, e.g. using Lloyd's algorithm (Du et al., 1999), real-time network  
573 updates including point deletion (Mostafavi et al., 2003), and network densification utilized in finite  
574 element mesh generation. These ~~two~~ operations, ~~i.e. change of nucleation point location and~~  
575 ~~network densification, may should~~ improve effectiveness of the proposed method by quick re-  
576 computation of the network and generation of more natural ~~the shape of for~~ navigable paths ~~in~~  
577 ~~such a way that more natural paths are generated~~. Enhancement of the navigable network in order  
578 to get obtain natural paths and quick network updates will be considered in future research.

579 Methods of alternative path-finding are currently under development in presented research. An  
580 alternative path may be understood in two ways: i) a path, which runs through a wall if all standard  
581 navigation routes through doors are blocked; ii) a path, which is longer than the shortest path and  
582 runs through standard navigation routes, but avoiding hazardous areas. In future work it is planned  
583 to include information about construction material in models and use it for more advanced egress  
584 route finding and simulations of hazard propagation in buildings.

585 The future work includes development of the decision support system based on VDN and the multi-  
586 attribute decision-making technique, which takes shortest, safest and simplest paths as input data  
587 and returns 'the best path'. The system will be suited for rescue ~~and emergency~~ teams, who need to  
588 get access to trapped people.



589 **Acknowledgment**

590 This research/publication was made possible by a National Priority Research Program NPRP award  
591 [NPRP-06-1208-2-492] from the Qatar National Research Fund (a member of The Qatar Foundation).  
592 The statements made herein are solely the responsibility of the author(s).

593 The authors are grateful to Prof. Chris Gold for discussion related to this work and his valuable  
594 suggestions.

595 **References**

- 596 Afyouni, I., Cyril, R. and Christophe, C., 2012. Spatial models for context-aware indoor navigation  
597 systems: A survey. *Journal of Spatial Information Science*, 1(4): 85--123.
- 598 Aurenhammer, F., 1991. Voronoi diagrams—a survey of a fundamental geometric data  
599 structure. *ACM Comput. Surv.*, 23(3): 345-405.
- 600 Axelsson, P., 2000. DEM Generation from Laser Scanner Data Using Adaptive TIN Models. In: D.  
601 Fritsch and M. Molenaar (Editors), XIXth ISPRS Congress. ISPRS, Amsterdam, The  
602 Netherlands, pp. 110-117.
- 603 Becker, T., Nagel, C. and Kolbe, T.H., 2009. A Multilayered space-event model for navigation in  
604 indoor spaces. *3D Geo-Information Sciences*: 61-77.
- 605 Boguslawski, P., 2011. Modelling and Analysing 3D Building Interiors with the Dual Half-Edge Data  
606 Structure. PhD Thesis, University of Glamorgan, Pontypridd, Wales, UK, 134 pp.
- 607 Boguslawski, P. and Gold, C., 2010. Euler Operators and Navigation of Multi-shell Building Models.  
608 In: T. Neutens and P. Maeyer (Editors), *Developments in 3D Geo-Information Sciences*.  
609 *Lecture Notes in Geoinformation and Cartography*. Springer, pp. 1-16.
- 610 Boguslawski, P. and Gold, C., 2015. Buildings and terrain unified – multidimensional dual data  
611 structure for GIS. *Geo-spatial Information Science*, 18(4): 151-158.
- 612 Boguslawski, P., Gold, C.M. and Ledoux, H., 2011. Modelling and analysing 3D buildings with a  
613 primal/dual data structure. *ISPRS Journal of Photogrammetry and Remote Sensing*, 66(2):  
614 188-197.
- 615 Brown, G., Nagel, C., Zlatanova, S. and Kolbe, T.H., 2013. Modelling 3D Topographic Space Against  
616 Indoor Navigation Requirements. In: J. Pouliot, S. Daniel, F. Hubert and A. Zamyadi (Editors),  
617 *Progress and New Trends in 3D Geoinformation Sciences*. Springer Berlin Heidelberg, Berlin,  
618 Heidelberg, pp. 1-22.
- 619 Chedid, R. and Najjar, N., 1996. Automatic finite-element mesh generation using artificial neural  
620 networks-Part I: Prediction of mesh density. *IEEE Transactions on Magnetics*, 32(5): 5173-  
621 5178.
- 622 DeCapua, C. and Bhaduri, B., 2007. Applications of Geospatial Technology in International Disasters  
623 and During Hurricane Katrina, Available at the Project Site of Capturing Hurricane Katrina  
624 Data For Analysis and Lessons-Learned Research  
625 ([www.gri.msstate.edu/research/katrinalessons/Documents/GeoSp\\_Tech\\_Applications.pdf](http://www.gri.msstate.edu/research/katrinalessons/Documents/GeoSp_Tech_Applications.pdf)).
- 626 Du, Q., Faber, V. and Gunzburger, M., 1999. Centroidal Voronoi Tessellations: Applications and  
627 Algorithms. *SIAM Review*, 41(4): 637-676.
- 628 Du, Q. and Gunzburger, M., 2002. Grid generation and optimization based on centroidal Voronoi  
629 tessellations. *Applied Mathematics and Computation*, 133(2–3): 591-607.
- 630 Dyck, D.N., Lowther, D.A. and McFee, S., 1992. Determining an approximate finite element mesh  
631 density using neural network techniques. *IEEE Transactions on Magnetics*, 28(2): 1767-1770.
- 632 Goetz, M. and Zipf, A., 2011. Formal definition of a user-adaptive and length-optimal routing graph  
633 for complex indoor environments. *Geo-spatial Information Science*, 14(2): 119-128.
- 634 Green, P.J. and Sibson, R., 1978. Computing Dirichlet Tessellations in the Plane. *The Computer*  
635 *Journal*, 21(2): 168-173.

636 Ho-Le, K., 1988. Finite element mesh generation methods: a review and classification. *Computer-*  
637 *Aided Design*, 20(1): 27-38.

638 Krūminaitė, M. and Zlatanova, S., 2014. Indoor space subdivision for indoor navigation, *Proceedings*  
639 *of the Sixth ACM SIGSPATIAL International Workshop on Indoor Spatial Awareness*. ACM,  
640 Dallas/Fort Worth, Texas, pp. 25-31.

641 Kuligowski, E.D.I., 10–11 June 2004. p. 68–90., 2004. Review of 28 egress models. In: R.D. Peacock  
642 and E.D. Kuligowski (Editors), *The workshop on building occupant movement during fire*  
643 *emergencies*, 10–11 June 2004. National Institute of Standards and Technology, pp. 66-88.

644 Kwan, M.-P. and Lee, J., 2005. Emergency response after 9/11: the potential of real-time 3D GIS for  
645 quick emergency response in micro-spatial environments. *Computers, Environment and*  
646 *Urban Systems*, 29: 93-113.

647 Lamarche, F. and Donikian, S., 2004. Crowd of Virtual Humans: a New Approach for Real Time  
648 Navigation in Complex and Structured Environments. *Computer Graphics Forum*, 23(3): 509-  
649 518.

650 Lee, J., 2004. A spatial access-oriented implementation of a 3-D GIS topological data model for urban  
651 entities. *Geoinformatica*, 8(3): 237-264.

652 Lee, J. and Kwan, M.P., 2005. A combinatorial data model for representing topological relations  
653 among 3D geographical features in micro-spatial environments. *International Journal of*  
654 *Geographical Information Science*, 19(10): 1039 - 1056.

655 Li, N., Becerik-Gerber, B., Krishnamachari, B. and Soibelman, L., 2014. A BIM centered indoor  
656 localization algorithm to support building fire emergency response operations. *Automation*  
657 *in Construction*, 42: 78-89.

658 Liu, L. and Zlatanova, S., 2011. A "door-to-door" path-finding approach for indoor navigation, *Gi4DM*  
659 *2011: GeoInformation for Disaster Management*. International Society for Photogrammetry  
660 and Remote Sensing (ISPRS), Antalya, Turkey.

661 Liu, L. and Zlatanova, S., 2012. Towards a 3D network model for indoor navigation. In: Zlatanova,  
662 Ledoux, Fendel and Rumor (Editors), *Urban and Regional Data Management*. UDMS Annual  
663 2011. CRCpress/Taylor and Francis Group, London, pp. 79-92.

664 Luo, F., Cao, G. and Li, X., 2014. An interactive approach for deriving geometric network models in  
665 3D indoor environments, *Proceedings of the Sixth ACM SIGSPATIAL International Workshop*  
666 *on Indoor Spatial Awareness*. ACM, Dallas/Fort Worth, Texas, pp. 9-16.

667 Mostafavi, M.A., Gold, C. and Dakowicz, M., 2003. Delete and insert operations in Voronoi/Delaunay  
668 methods and applications. *Computers & Geosciences*, 29(4): 523-530.

669 Nelson, H.E. and MacLennan, H.A., 1995. Emergency Movement. In: P.J. DiNenno, C.L. Beyler, R.L.P.  
670 Custer, W.D. Walton, J.M. Watts, D. Drysdale and J.R. Hall (Editors), *SFPE handbook of fire*  
671 *protection engineering*. Society of Fire Protection Engineers, Boston, MA, USA and National  
672 Fire Protection Association, Quincy, MA, USA, pp. 3/286-3/295.

673 OGC, 2014. OGC IndoorGML. Open Geospatial Consortium Inc.

674 Pauls, J., 1995. Movement of people. In: P.J. DiNenno, C.L. Beyler, R.L.P. Custer, W.D. Walton, J.M.  
675 Watts, D. Drysdale and J.R. Hall (Editors), *SFPE handbook of fire protection engineering*.  
676 Society of Fire Protection Engineers, Boston, MA, USA and National Fire Protection  
677 Association, Quincy, MA, USA, pp. 3/263-3/285.

678 Petersen, S.B. and Martins, P.A.F., 1997. FINITE ELEMENT REMESHING: A METAL FORMING  
679 APPROACH FOR QUADRILATERAL MESH GENERATION AND REFINEMENT. *International*  
680 *Journal for Numerical Methods in Engineering*, 40(8): 1449-1464.

681 Scharfenort, N., 2012. Urban Development and Social Change in Qatar: The Qatar National Vision  
682 2030 and the 2022 FIFA World Cup. *Journal of Arabian Studies*, 2(2): 209-230.

683 Stoffel, E.P., Lorenz, B. and Ohlbach, H.J., 2007. Towards a Semantic Spatial Model for Pedestrian  
684 Indoor Navigation *Advances in Conceptual Modeling – Foundations and Applications*.  
685 *Lecture Notes in Computer Science*, pp. 328-337.

686 Stroud, I., 2006. *Boundary Representation Modelling Techniques*. Springer-Verlag, New York.

- 687 Tashakkori, H., Rajabifard, A. and Kalantari, M., 2015. A new 3D indoor/outdoor spatial model for  
688 indoor emergency response facilitation. *Building and Environment*, 89: 170-182.
- 689 Vanclooster, A., De Maeyer, P., Fack, V. and Van de Weghe, N., 2014. Calculating Least Risk Paths in  
690 3D Indoor Space. In: U. Isikdag (Editor), *Innovations in 3D Geo-Information Sciences. Lecture  
691 Notes in Geoinformation and Cartography*. Springer International Publishing, pp. 13-31.
- 692 Wallgrün, J., 2005. Autonomous Construction of Hierarchical Voronoi-Based Route Graph  
693 Representations. In: C. Freksa, M. Knauff, B. Krieg-Brückner, B. Nebel and T. Barkowsky  
694 (Editors), *Spatial Cognition IV. Reasoning, Action, Interaction. Lecture Notes in Computer  
695 Science*. Springer Berlin Heidelberg, pp. 413-433.
- 696 Wang, Z. and Zlatanova, S., 2013. Taxonomy of Navigation for First Responders. In: M.J. Krisp  
697 (Editor), *Progress in Location-Based Services*. Springer Berlin Heidelberg, Berlin, Heidelberg,  
698 pp. 297-315.
- 699 Wenjie, Y. and Schneider, M., 2010. Supporting Continuous Range Queries in Indoor Space, Eleventh  
700 International Conference on Mobile Data Management (MDM), pp. 209-214.
- 701 Yang, L. and Worboys, M., 2015. Generation of navigation graphs for indoor space. *International  
702 Journal of Geographical Information Science*, 29(10): 1737–1756.
- 703 Zhang, J. and Lin, X., 2013. Filtering airborne LiDAR data by embedding smoothness-constrained  
704 segmentation in progressive TIN densification. *ISPRS Journal of Photogrammetry and  
705 Remote Sensing*, 81: 44-59.
- 706 Zverovich, V., Mahdjoubi, L., Boguslawski, P., Fadli, F. and Barki, H., 2016. Emergency Response in  
707 Complex Buildings: Automated Selection of Safest and Balanced Routes. *Computer-Aided  
708 Civil and Infrastructure Engineering*.

709

710